

Novel Universality Classes in Ferroelectric Liquid Crystals

Amit K Chattopadhyay

*Aston University, System Analytics Research Institute, Birmingham, B4 7ET, UK**

Prabir K. Mukherjee

*Department of Physics, Government College of Engineering and Textile Technology,
12 William Carey Road, Serampore, Hooghly-712201, India*

Starting from a Langevin formulation of a thermally perturbed nonlinear elastic model of the ferroelectric smectic-C* (SmC*) liquid crystals in the presence of an electric field, this article characterizes the hitherto unexplored dynamical phase transition from a thermo-electrically forced ferroelectric SmC* phase to a chiral nematic liquid crystalline phase and vice versa. The theoretical analysis is based on a combination of dynamic renormalization (DRG) and numerical simulation of the emergent model. While the DRG architecture predicts a generic transition to the Kardar-Parisi-Zhang (KPZ) universality class at dynamic equilibrium, in agreement with recent experiments, the numerical simulations of the model show simultaneous existence of two phases, one a “subdiffusive” (SD) phase characterized by a dynamical exponent value of 1, and the other a KPZ phase, characterized by a dynamical exponent value of 1.5. The SD phase flows over to the KPZ phase with increased external forcing, offering a new universality paradigm, hitherto unexplored in the context of ferroelectric liquid crystals.

PACS numbers: 61.30.-v,05.10.Gg,05.10.Cc

arXiv:1705.08705v1 [cond-mat.soft] 24 May 2017

* a.k.chattopadhyay@aston.ac.uk

INTRODUCTION

Kardar-Parisi-Zhang (KPZ) equation [1–4] has long been proposed as a paradigmatic model characterizing the statistical properties of a growing interface. While the model itself is a pure theorist’s delight, in that it offers both weak and strong coupling regimes with transitions in between, a field theoretic paradise of sorts, from an experimental perspective, the model has often been looked down upon apart from rare conjectures and interpolations [5, 6].

On the other hand, researches on smectic-A to SmC* (SmA-SmC*) phase transitions have been going on over the past few decades. Now there is also an increasing interest in the chiral nematic (N*) to SmC* (N*-SmC*) phase transitions, both because of their inherent challenge [7] as also due to the application potentials [8]. These studies have generally relied on deterministic free energy based descriptions and follow-up estimations without much importance ascribed to the inherent thermal or boundary fluctuations surrounding the samples concerned. When such thermally forced stochastic perturbations are considered, the liquid crystalline phases may indeed transgress their conventional regimes and cross over to hitherto unexplored (“hidden”) regimes, as recently shown in [9]. I

The present work studies the impact of stochastic fluctuations in modifying the spatiotemporal properties of cholesteric liquid crystals in the presence of a random magnetic field. Our results show that stochastic fluctuations drive the system to a Kosterlitz-Thouless transition point, through a second-order phase transition, thereby converging to a Kardar-Parisi-Zhang universality class. For weaker ramping forces, the system converges to a non-KPZ fixed point.

Such mapping to established universality classes is unlikely to be restricted to only one or two specific cases, which is why there has been an upsurge in interest in stochastic modeling from the perspective of analyzing some dynamical propagation fronts and related crossovers and/or phase transitions in liquid crystalline systems [9–14]. Such phase transitions range from geometric phases [15] to isotropic-nematic-columnar phases [16, 17]. Nematic liquid crystal turbulence has been shown to exhibit a clear Kardar-Parisi-Zhang (KPZ)-class behavior [10, 11]. Takeuchi and Sano [10, 11] experimentally studied the scale-invariant fluctuations of growing interfaces in nematic liquid-crystal turbulence. They observed that the interfaces exhibit self-affine roughening characterized by both spatial and temporal scaling laws of the KPZ theory in 1+1 dimensions. Golubovic and Wang [12, 13] found a theoretical relationship between the fluctuations of smectic-A to fluctuations KPZ dynamical model. They observed that the KPZ model in 2+1 dimensions maps into a elastic critical point of 3D Smectic-A with broken inversion symmetry (ferroelectric smectic-A).

Here we report on what we believe to be the first theoretical study of the dynamical evolution patterns of ferroelectric smectic-C* (SmC*) liquid crystals in an electric field, using firstly the language of dynamic renormalization group (DRG), which we later complement with numerical simulation of the propounded stochastic model. Both analytical (DRG based) and numerical (simulation) results predict a chiral nematic (N*) to SmC* phase transition. In the experimentally viable low frequency limit, our dynamical model predicts the onset of a Kosterlitz-Thouless transition. At large enough spatiotemporal scales, the inherent nonlinearity drives the system to a Kardar-Parisi-Zhang fixed point, theoretically represented by appropriate self-affine scaling.

THE THEORETICAL MODEL

The inner fabric of our proposed model relies on the nonlinear elastic model of SmC* liquid crystal in the presence of an electric field. The SmC* phase has a helical structure where the director field tilts from the layer normal by θ and rotates along normal direction. An electric polarization appears in the plane parallel with the layer and makes a right angle along the director field and in the result it rotates along the layer normal. By applying the electric field in a direction parallel to the layer, the helical structure is unwound due to a coupling between the electric field and the polarization. We assume all elastic constants equal, define a two dimensional director in the plane of the layers. So the the director \mathbf{n} is defined as: $n_x = \sin \theta \cos \phi(z)$, $n_y = \sin \theta \sin \phi(z)$. $n_z = \cos \theta$. $\phi(z)$ is the azimuthal angle between \mathbf{n} and y axis and is thus z dependent. θ is the tilt angle between the layer normal and the director \mathbf{n} and does not vary with z. Here layer normal is assumed to be in the z direction. In what follows, we first define a Frank free energy, as shown in Eq. (1) below. This is then followed by a Langevin formulation, starting from this free energy, to model the time dynamics of this system. We shall restrict our interest to a one dimensional dynamical problem in space.

The Frank Free Energy

Based on the Cladis-Saarloos formalism [18], the free energy of the SmC* phase in an applied electric field $\mathbf{E} = E(0, 1, 0)$ can be written as

$$g = \int \left[\frac{K\theta^2}{2} \left(\frac{d\phi}{dz} + q_0 \right)^2 - \frac{\epsilon_a \theta^2}{8\pi} E^2 \sin^2 \phi - P\theta E \cos \phi \right] dz, \quad (1)$$

where K is the twist elastic constant, q_0 the wave vector corresponding to $E = 0$ ($q_0 = 2\pi/\lambda_0$). ϵ_a is the liquid crystal dielectric anisotropy. P is the polarization. We assume polarization P rotates about the z axis and the electric field is applied in the y direction. The above free energy (1) was extensively studied by Cladis and Saarloos [18] to discuss the various forms of front propagation of the SmC* state. The functional integral shown in Eq. (1) above can be approximately solved in certain cases using a saddle point approximation method but this will not work in the non-asymptotic regime, the focal point of our interest [19].

The Langevin Model

The free energy defined in Eq. (1) can be used to arrive at the stochastic Langevin description, as presented in Risken [20]. The time dependent Ginzburg-Landau (TDGL)-type model can then be specified by the following Langevin dynamics

$$M \frac{\partial \phi(z, t)}{\partial t} = - \frac{\delta g}{\delta \phi} + F_0 + \eta(z, t), \quad (2)$$

where $\eta(z, t)$ is a stochastic white noise represented by $\langle \eta(z, t) \eta(z', t') \rangle = D_0 \delta(z - z') \delta(t - t')$ and $\langle \eta(z, t) \rangle = 0$, in which the curly brackets “ $\langle \rangle$ ” represent ensemble average over all noise realizations and D_0 is the noise strength, a constant, while $\frac{\delta g}{\delta \phi}$ is the functional derivative of g with respect to variable ϕ . F_0 is a constant overdamped force that pumps a steady energy into the system. Such a term is related to the existence of a kinetic roughening in the model that can only be counter- balanced by a negative damping term F_0 .

Eq. (2) can then be rewritten as

$$M \frac{\partial \phi}{\partial t} = \frac{\epsilon_a \theta^2 E^2}{8\pi} \sin 2\phi - P\theta E \sin \phi + K\theta^2 \frac{\partial^2 \phi}{\partial z^2} + F_0 + \eta(z, t). \quad (3)$$

The above Eq. (3) represents a quintessential sine-Gordon model [21] whose low frequency spatiotemporal scaling properties have been studied previously by Chattopadhyay [22], an approach that was later implemented in analyzing a class of liquid crystals by Chattopadhyay and Mukherjee [9].

We will now calculate the renormalization group (RG) flows for the dynamical nonlinear model presented in Eq. (3) above. In order to achieve a scale independent formulation of the aforementioned dynamics, in the following, we rescale the starting model variable on a periodic lattice using the transformation $h = \frac{a}{2\pi} \phi$, which then leads to the following representation:

$$\eta \frac{\partial h}{\partial t} = \gamma \frac{\partial^2 h}{\partial z^2} - \frac{2\pi V_1}{a} \sin \left(\frac{2\pi h}{a} \right) + \frac{2\pi V_2}{a} \sin \left(\frac{4\pi h}{a} \right) + F + N(z, t). \quad (4)$$

Here the rescaled parameters are given by $\eta = \frac{M}{K}$, $\gamma = \theta^2$, $\frac{2\pi V_1}{a} = \frac{P\theta E a}{2\pi K}$, $\frac{2\pi V_2}{a} = \frac{\epsilon_a \theta^2 E^2 a}{16\pi^2 K}$, $F = \frac{F_0 a}{2\pi K}$ and the rescaled noise $N(z, t) = \frac{a\eta'(z, t)}{2\pi K}$. The model above is a generalized extension of the classic noisy sine-Gordon model that can be studied using the method previously used by Chattopadhyay [22] and later contextualized for liquid crystals in [9], in which the second moment of the noise-noise correlation in the k -space can be given by

$$\langle N(k, t) N(k', t') \rangle = 2Df \left(\frac{\pi k}{\Lambda} \right) \delta(k + k') \delta(t - t'), \quad (5)$$

where $f(1 - x) = \theta(x)$, a Heaviside step function, $\Lambda \propto \frac{\pi}{a}$, and the rescaled noise strength $D = D_0 \frac{a^2}{4\pi^2 K^2}$ is defined through the fluctuation-dissipation theorem [23] as $D \propto \eta T$, where T is the “non-equilibrium temperature” [24].

RESULTS

Eq. (4) defines a stochastically evolving structure which we solve independently using two well established architectures - first, using the Dynamic Renormalization Group (DRG) approach and second, a thorough numerical solution of the same stochastic model using appropriate discretization that simultaneously offers a complementary strand to the DRG method while also probing regimes that go beyond the perturbative mechanism accorded under the DRG auspice. Note that ours being a stochastically perturbed 1+1 dimensional model, it is open to phase transition possibilities.

The Dynamic Renormalization Group Analysis

The model presented in Eqs. (4-5) is the d=1+1 dimensional version of the Nozieres-Gallet [21] or Rost-Spohn model [27] for the special case of $\lambda = 0$. In the following analysis, we will employ the same dynamic renormalization group (DRG) prescription as in [27]. Our effective dynamical equation for the description is the following:

$$\eta \frac{\partial h}{\partial t} = \gamma \frac{\partial^2 h}{\partial z^2} - \frac{2\pi V_1}{a} \sin\left(\frac{2\pi h}{a}\right) + \frac{2\pi V_2}{a} \sin\left(\frac{4\pi h}{a}\right) + F + \frac{\lambda}{2} \left(\frac{\partial h}{\partial z}\right)^2 + N(z, t), \quad (6)$$

where the KPZ nonlinearity $\frac{\lambda}{2} \left(\frac{\partial h}{\partial z}\right)^2$ has been added in advance, in recognition of the same term appearing after the renormalization, as studied in [9, 27]. All other terms bear the same meaning as in Eq. (4) before.

The fast frequency components are integrated over the momentum shell $\Lambda e^{-\Delta l} < |k| < \Lambda$ i.e. $\Lambda(1 - \Delta l)$ for $< |k| < \Lambda$, in the limit of infinitesimally small Δl . We assume both V_1 and V_2 are perturbative constants.

Within this momentum shell, the variables are renormalized as follows: $k \rightarrow k' = (1 + \Delta l)k$, $z \rightarrow z' = (1 - \Delta l)z$, $h \rightarrow h' = h$, $t \rightarrow t' = (1 - 2\Delta l)t$, $\eta \rightarrow \eta' = \eta$, $\gamma \rightarrow \gamma' = \gamma$, $V_1 \rightarrow V_1' = (1 + 2\Delta l)V_1$, $V_2 \rightarrow V_2' = (1 + 2\Delta l)V_2$, $F \rightarrow F' = (1 + 2\Delta l)F$ and $\lambda \rightarrow \lambda' = \lambda$.

First we discuss the perturbative dynamics. In this case Eq. (6) can be rewritten as

$$\eta \frac{\partial h}{\partial t} = \gamma \frac{\partial^2 h}{\partial z^2} + \Psi(h) + N, \quad (7)$$

where $\Psi(h) = -\frac{2\pi V_1}{a} \sin\left[\frac{2\pi}{a}\left(h + \frac{Ft}{\eta}\right)\right] + \frac{2\pi V_2}{a} \sin\left[\frac{4\pi}{a}\left(h + \frac{Ft}{\eta}\right)\right] + \frac{\lambda}{2} \left(\frac{\partial h}{\partial z}\right)^2$.

Using perturbation expansions for the dynamic variables $X_i = h, N$, we can write $N = \bar{N} + \delta N$, where the quantity \bar{N} is defined within the momentum range $|k| < (1 - \Delta l)\Lambda$, with δN defined inside the annular ring $(1 - \Delta l)\Lambda < |k| < \Lambda$, to get

$$\begin{aligned} \eta \frac{\partial \bar{h}}{\partial t} &= \gamma \frac{\partial^2 \bar{h}}{\partial z^2} + \bar{\Psi}(\bar{h}, \delta h) + \bar{N}, \\ \eta \frac{\partial \delta h}{\partial t} &= \gamma \frac{\partial^2 \delta h}{\partial z^2} + \delta \Psi(\bar{h}, \delta h) + \delta N, \end{aligned} \quad (8)$$

where $\bar{\Psi} = \langle \Psi \rangle_{\delta N}$, averaging defined over all noise perturbations. $\bar{\Psi}$ and $\delta \Psi$ can be expressed as

$$\begin{aligned} \bar{\Psi} &= -\frac{2\pi V_1}{a} \sin\left[\frac{2\pi}{a}\left(\bar{h} + \frac{Ft}{\eta}\right)\right] \left(1 - \frac{2\pi^2}{a^2} \langle \delta h^2 \rangle_{\delta N}\right) + \frac{2\pi V_2}{a} \sin\left[\frac{4\pi}{a}\left(\bar{h} + \frac{Ft}{\eta}\right)\right] \left(1 - \frac{8\pi^2}{a^2} \langle \delta h^2 \rangle_{\delta N}\right) \\ &\quad + \frac{\lambda}{2} \left(\frac{\partial \bar{h}}{\partial z}\right)^2 + \frac{\lambda}{2} \langle \left(\frac{\partial \delta h}{\partial z}\right)^2 \rangle_{\delta N} \\ \delta \Psi &= \left\{ -\frac{4\pi^2 V_1}{a^2} \cos\left[\frac{2\pi}{a}\left(\bar{h} + \frac{Ft}{\eta}\right)\right] + \frac{8\pi^2 V_2}{a^2} \cos\left[\frac{4\pi}{a}\left(\bar{h} + \frac{Ft}{\eta}\right)\right] \right\} \delta h + \lambda \left(\frac{\partial \bar{h}}{\partial z}\right) \cdot \left(\frac{\partial \delta h}{\partial z}\right). \end{aligned} \quad (9)$$

Expanding $\delta h = \delta h^{(0)} + \delta h^{(1)} + \dots$ perturbatively, in the Fourier transformed k -space, we get

$$\delta h^{(0)}(z, t) = \int_{-\infty}^t dt' \int dz' G_0(z - z', t - t') \delta N(z', t') \quad (10)$$

and

$$\begin{aligned} \delta h^{(1)}(z, t) = & \int_{-\infty}^t dt' \int dz' G_0(z - z', t - t') \times \left[-\frac{4\pi^2 V_1}{a^2} \cos\left(\frac{2\pi}{a}(\bar{h}(z', t') + \frac{Ft'}{\eta})\right) \right. \\ & \left. + \frac{8\pi^2 V_2}{a^2} \cos\left(\frac{4\pi}{a}(\bar{h}(z', t') + \frac{Ft'}{\eta})\right) \right] \delta h^{(0)} + \lambda \left(\frac{\partial \bar{h}(z', t')}{\partial z'} \right) \left(\frac{\partial \delta h^{(0)}(z', t')}{\partial z'} \right), \end{aligned} \quad (11)$$

where $G_0(x, t) = \frac{1}{2\pi\gamma t} e^{-\frac{\eta x^2}{2\gamma t}}$ is the Green's function. For the initial condition $h(z, t = -\infty) = 0$, we get

$$\langle (\delta h)^2(z, t) \rangle = \langle (\delta h^{(0)})^2 \rangle + 2 \langle \delta h^{(0)}(z, t) \delta h^{(1)}(z, t) \rangle \quad (12)$$

and

$$\langle (\partial_z \delta h)^2(z, t) \rangle = \langle (\partial_z \delta h^{(0)})^2 \rangle + 2 \langle \partial_z \delta h^{(0)} \partial_z \delta h^{(1)} \rangle. \quad (13)$$

Using Eqs. (10-13), we can now write

$$\delta h_k(t) = \frac{1}{\eta} e^{-\frac{\gamma}{\eta} k^2 t} \int_{-\infty}^t dt' \delta N_k(t') e^{\frac{\gamma}{\eta} k^2 t'} \quad (14)$$

The corresponding correlation functions are given by

$$\left\langle \delta h^{(0)}(z, t) \delta h^{(0)}(z', t') \right\rangle = \frac{D}{\gamma\eta} e^{i\Lambda(z-z')} e^{-\frac{\gamma}{\eta} \Lambda^2 |t-t'|} \Delta l \quad \text{and} \quad (15)$$

$$\left\langle \left(\frac{\partial \delta h^{(0)}(z, t)}{\partial z} \right) \left(\frac{\partial \delta h^{(0)}(z', t')}{\partial z'} \right) \right\rangle = -\frac{D}{\gamma\eta} \Lambda^2 e^{i\Lambda(z-z')} e^{-\frac{\gamma}{\eta} \Lambda^2 |t-t'|} \Delta l, \quad (16)$$

where $D = \frac{a^2}{4\pi^2 K^2} \eta T$.

Dynamic Renormalization Group Flow Equations

The Dynamic Renormalization Group (DRG) flow equations, correct up to the first order, can be shown to be as follows:

$$dV_1^{(l)} = -\frac{2\pi^2}{a^2} \langle \delta h^{(0)2}(z, t) \rangle = -\frac{\eta T}{2\gamma\eta K^2} \Delta l, \quad (17)$$

$$dV_2^{(l)} = -\frac{8\pi^2}{a^2} \langle \delta h^{(0)2}(z, t) \rangle = -\frac{2\eta T}{\gamma\eta K^2} \Delta l, \quad (18)$$

$$dF^{(l)} = \frac{\lambda}{2} \left\langle \left(\frac{\partial \delta h^{(0)}}{\partial z} \right)^2 \right\rangle_{\delta N} = \frac{\lambda T}{2\pi\gamma} \Lambda^2 \Delta l. \quad (19)$$

We now obtain the first order dynamic renormalization group (DRG) flows for V and F .

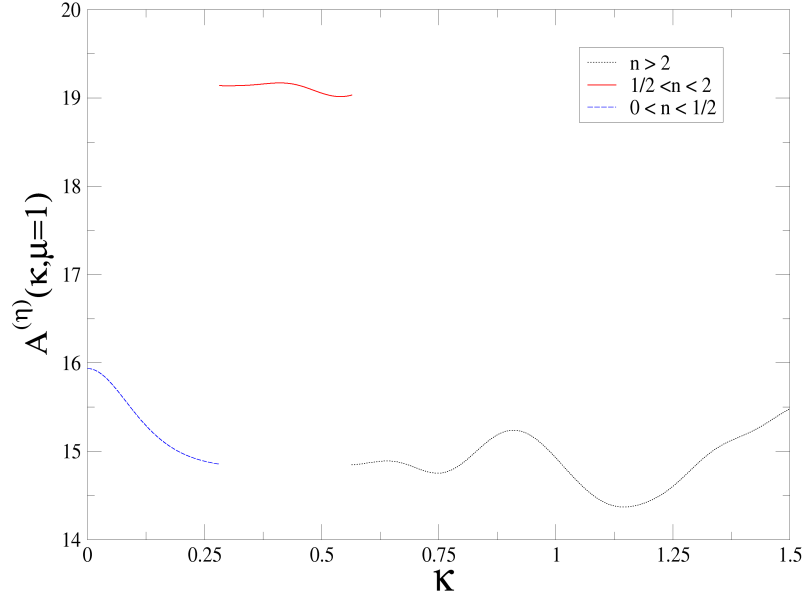


FIG. 1. Variation of the DRG flow integral $A_\mu^{(\eta)}(n; \kappa)$ with renormalized force κ for $\mu = 1$. The discontinuity observed between $0.25 < \kappa < 0.5$ is a signature of the phase transition to the KPZ phase.

In order to calculate the DRG flows for γ , η and D , we need to evaluate the second ordered corrections terms $\langle \delta h^{(0)} \delta h^{(1)} \rangle$ and $\langle \partial \delta h^{(0)} \partial \delta h^{(1)} \rangle$. Starting from the free energy representation Ψ is Eq. (9), these two-point correlation functions, accurate up to second-order in perturbation, are presented below:

$$\begin{aligned}
\left\langle \delta h^{(0)}(z, t) \delta h^{(1)}(z, t) \right\rangle &= -\frac{4\pi^2 V_1}{a^2} \int_{-\infty}^t dt' \int dz' \cos \left[\frac{2\pi}{a} \left(\bar{h} + \frac{Ft'}{\eta} \right) \right] G_0(z - z', t - t') \\
&\quad \times \langle \delta h^{(0)}(z, t) \delta h^{(0)}(z', t') \rangle \\
&\quad + \frac{8\pi^2 V_2}{a^2} \int_{-\infty}^t dt' \int dz' \cos \left[\frac{4\pi}{a} \left(\bar{h} + \frac{Ft'}{\eta} \right) \right] G_0(z - z', t - t') \\
&\quad \times \langle \delta h^{(0)}(z, t) \delta h^{(0)}(z', t') \rangle,
\end{aligned} \tag{20a}$$

and

$$\begin{aligned}
\left\langle \left(\frac{\partial \delta h^{(0)}(z, t)}{\partial z} \right) \left(\frac{\partial \delta h^{(1)}(z', t')}{\partial z'} \right) \right\rangle &= \frac{\eta}{2\gamma} \int_{-\infty}^t dt' \int dz' G_0(z - z', t - t') - \left(\frac{z' - z}{t - t'} \right) \\
&\times \left\{ -\frac{4\pi^2 V_1}{a^2} \cos \left[\frac{2\pi}{a} \left(\bar{h}(z', t') + \frac{Ft'}{\eta} \right) \right] + \frac{8\pi^2 V_2}{a^2} \cos \left[\frac{4\pi}{a} \left(\bar{h}(z', t') + \frac{Ft'}{\eta} \right) \right] \right\} \times \left\langle \left(\frac{\partial \delta h^{(0)}(z, t)}{\partial z} \right) \left(\frac{\partial \delta h^{(0)}(z', t')}{\partial z'} \right) \right\rangle_{\delta N} \\
&+ \frac{\eta\lambda}{\gamma} \int_{-\infty}^t dt' \int dz' \left(-\frac{z' - z}{t - t'} \right) \frac{\partial h(z', t')}{\partial z} G_0(z - z', t - t') \left\langle \left(\frac{\partial \delta h^{(0)}(z, t)}{\partial z} \right) \left(\frac{\partial \delta h^{(0)}(z', t')}{\partial z'} \right) \right\rangle_{\delta N}.
\end{aligned} \tag{20b}$$

The representation in Eqs. (20a, 20b) provide the detailed form of the (second-order) perturbed sine-Gordon Hamiltonian:

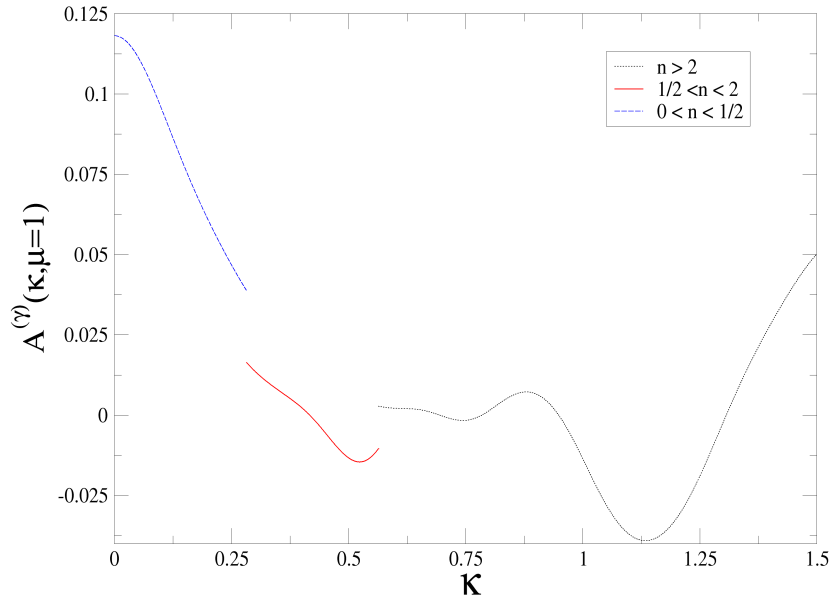


FIG. 2. Variation of the DRG flow integral $A_{\mu}^{(\gamma)}(n; \kappa)$ with renormalized force κ for $\mu = 1$. The discontinuity observed between $0.25 < \kappa < 0.5$ is a signature of the phase transition to the KPZ phase.

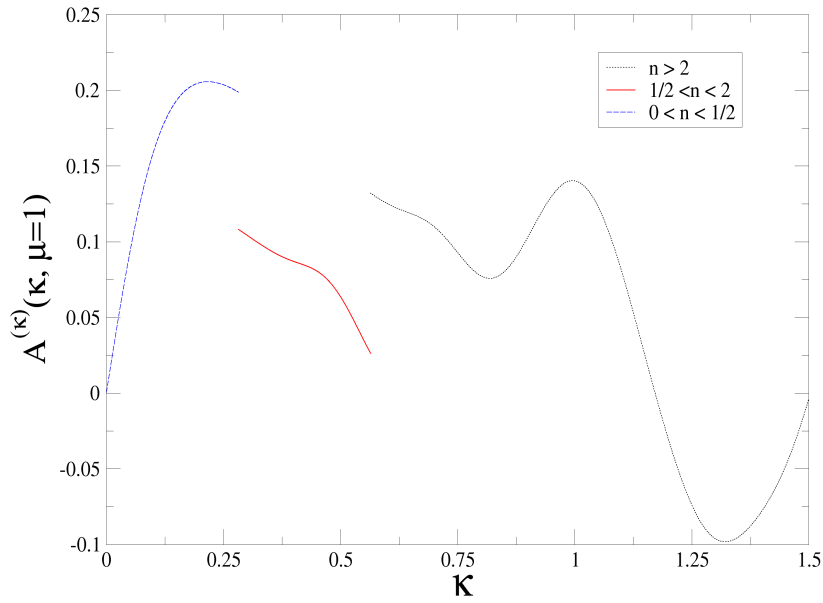


FIG. 3. Variation of the DRG flow integral $A_{\mu}^{(\kappa)}(n; \kappa)$ with renormalized force κ for $\mu = 1$. The discontinuity observed between $0.25 < \kappa < 0.5$ is a signature of the phase transition to the KPZ phase.

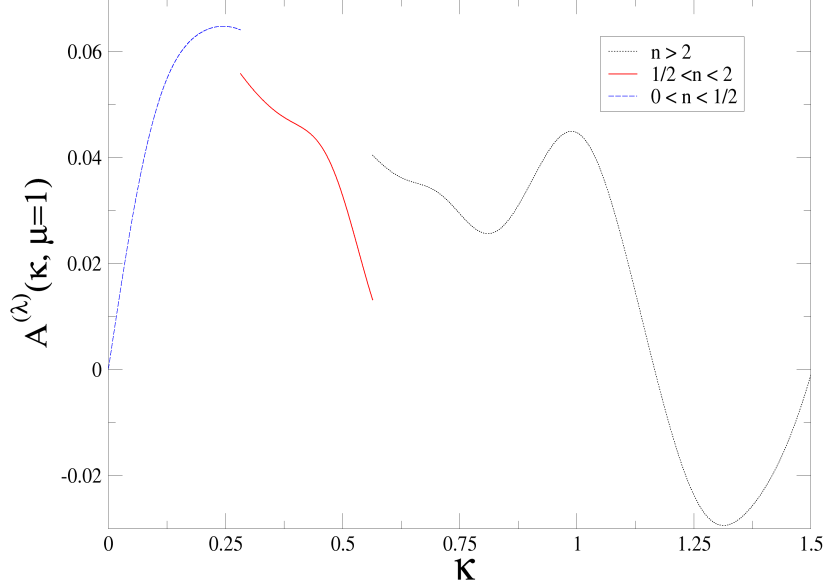


FIG. 4. Variation of the DRG flow integral $A_{\mu}^{(\lambda)}(n; \kappa)$ with renormalized force κ for $\mu = 1$. The discontinuity observed between $0.25 < \kappa < 0.5$ is a signature of the phase transition to the KPZ phase.

$$\begin{aligned}
\Psi_{SG} \approx & -\frac{8\pi^3 V_1^2 T}{\gamma^2 a^5} \left(\frac{a^2}{4\pi^2 K^2} \right) \Delta l \int_{-\infty}^t \frac{dt'}{t-t'} \int dz' e^{i\Lambda|z-z'|} \times e^{-[\frac{\gamma}{2\eta} \frac{(z-z')^2}{(t-t')} - \frac{\gamma}{\eta} \Lambda^2(t-t') - \frac{2\pi^2}{a^2} \langle [\bar{h}(z,t) - \bar{h}(z',t')]^2 \rangle_{\delta N}]} \\
& \times \left[\frac{2\pi}{a} \left(\frac{\partial}{\partial t} \bar{h}(z,t)(t-t') - \frac{1}{2} \frac{\partial^2 \bar{h}(z,t)}{\partial z^2} (z-z')^2 \right) \right. \\
& \times \cos \left(\frac{2\pi F}{a \eta} (t-t') \right) + \left(1 - \frac{2\pi^2}{a^2} \left(\frac{\partial \bar{h}(z,t)}{\partial z} \right)^2 (z-z')^2 \right) \times \sin \left(\frac{2\pi F}{a \eta} (t-t') \right) \left. \right] \\
& - \frac{64\pi^3 V_2^2 T}{\gamma^2 a^5} \left(\frac{a^2}{4\pi^2 K^2} \right) \xi \Delta l \int_{-\infty}^t \frac{dt'}{t-t'} \int dz' e^{i\Lambda|z-z'|} \times e^{-[\frac{\gamma}{2\eta} \frac{(z-z')^2}{(t-t')} - \frac{\gamma}{\eta} \Lambda^2(t-t') - \frac{8\pi^2}{a^2} \langle [\bar{h}(z,t) - \bar{h}(z',t')]^2 \rangle_{\delta N}]} \\
& \times \left[\frac{4\pi}{a} \left(\frac{\partial}{\partial t} \bar{h}(z,t)(t-t') - \frac{1}{2} \frac{\partial^2 \bar{h}(z,t)}{\partial z^2} (z-z')^2 \right) \right. \\
& \times \cos \left(\frac{4\pi F}{a \eta} (t-t') \right) + \left(1 - \frac{8\pi^2}{a^2} \left(\frac{\partial \bar{h}(z,t)}{\partial z} \right)^2 (z-z')^2 \right) \times \sin \left(\frac{4\pi F}{a \eta} (t-t') \right) \left. \right]. \tag{21}
\end{aligned}$$

The terms in Eq. (21) that are respectively proportional to $\frac{\partial \bar{h}}{\partial t}$, $\partial_i \partial_j \bar{h}$ and $(\partial_i \bar{h})^2$ are the renormalized contributions for η , γ and a new KPZ nonlinearity term λ that automatically gets created from a sine-Gordon potential. This drives the dynamics to the KPZ fixed point with the constant term above renormalizing the ramping force F .

Combining information from Eqs. (20a, 20b, 21), the DRG flow equations can be outlined as follows:

$$\frac{dU_1}{dl} = (2-n)U_1, \tag{22}$$

$$\frac{dU_2}{dl} = (2-4n)U_2, \tag{23}$$

$$\frac{d\gamma}{dl} = \frac{8\pi^4}{\gamma a^4} n A_1^{(\gamma)}(n; \kappa) U_1^2 + \frac{64\pi^4}{\gamma a^4} n A_2^{(\gamma)}(n; \kappa) U_2^2, \quad (24)$$

$$\frac{d\eta}{dl} = \frac{32\pi^4}{\gamma a^4} \frac{\eta}{\gamma} n A_1^{(\eta)}(n; \kappa) U_1^2 + \frac{256\pi^4}{\gamma a^4} \frac{\eta}{\gamma} n A_2^{(\eta)}(n; \kappa) U_2^2 \quad (25)$$

$$\frac{d\lambda}{dl} = \frac{32\pi^5}{\gamma a^5} n A_1^{(\lambda)}(n; \kappa) U_1^2 + \frac{256\pi^5}{\gamma a^5} n A_2^{(\lambda)}(n; \kappa) U_2^2, \quad (26)$$

$$\frac{dD}{dl} = \frac{32\pi^4}{\gamma a^4} \frac{D}{\gamma} n A_1^{(\eta)}(n; \kappa) U_1^2 + \frac{256\pi^4}{\gamma a^4} \frac{D}{\gamma} n A_2^{(\eta)}(n; \kappa) U_2^2 + \frac{1}{4\pi} \frac{D^2 \lambda^2}{\gamma^3} \quad (27)$$

$$\frac{dK}{dl} = 2K - \frac{8\pi^3}{\gamma a^3} n A_1^{(K)}(n; \kappa) U_1^2 - \frac{64\pi^3}{\gamma a^3} n A_2^{(K)}(n; \kappa) U_2^2 + \frac{D}{2\pi\eta\gamma} \lambda, \quad (28)$$

where $U_\mu = V_\mu/\Lambda^2$ ($\mu = 1, 2$), $K = F/\Lambda^2$, $\bar{\rho} = \Lambda\rho$, $x = \frac{\gamma(t-t')}{\eta\rho^2}$, $D = \frac{a^2}{4\pi^2 K^2} \eta T$, $n = \frac{2\pi D}{\gamma a^2} (\frac{a^2}{4\pi^2 K^2})$ and $\kappa = \frac{2\pi K}{a\gamma}$.

The functional forms of the DRG flow integrals $A^{(\gamma)}(n; \kappa)$, $A^{(\eta)}(n; \kappa)$, $A^{(\lambda)}(n; \kappa)$ and $A^{(K)}(n; \kappa)$ are defined as follows:

$$A_\mu^{(\gamma)}(n; \kappa) = \int_0^\infty \frac{dx}{x} \int_0^\infty d\bar{\rho} \bar{\rho}^2 e^{i\bar{\rho}} \cos\left(\frac{2\pi\mu}{a} \frac{Kx\bar{\rho}^2}{\gamma}\right) e^{-f_\mu}, \quad (29)$$

$$A_\mu^{(\eta)}(n; \kappa) = \frac{x}{\bar{\rho}^2} A_\mu^{(\gamma)}(n; \kappa), \quad (30)$$

$$A_\mu^{(\lambda)}(n; \kappa) = \int_0^\infty \frac{dx}{x} \int_0^\infty d\bar{\rho} \bar{\rho}^2 e^{i\bar{\rho}} \sin\left(\frac{2\pi\mu}{a} \frac{Kx\bar{\rho}^2}{\gamma}\right) e^{-f_\mu}, \quad (31)$$

$$A_\mu^{(K)}(n; \kappa) = \frac{1}{\bar{\rho}^2} A_\mu^{(\lambda)}(n; \kappa), \quad (32)$$

where the components can be estimated from the following identities

$$\begin{aligned} f_1 &= \frac{1}{2x} + x\bar{\rho}^2 + \frac{2\pi D}{\gamma a^2} \chi(\bar{\rho}, x), \\ f_2 &= \frac{1}{2x} + x\bar{\rho}^2 + \frac{8\pi D}{\gamma a^2} \chi(\bar{\rho}, x), \\ \chi(|z-z'|, |t-t'|) &= \frac{\pi\gamma}{\eta T} \langle [\bar{h}(z, t) - \bar{h}(z', t')]^2 \rangle_{\bar{N}}, \\ \langle [\bar{h}(z, t) - \bar{h}(z', t')]^2 \rangle_{\bar{N}} &= \frac{\eta T}{\pi\gamma} \int_0^1 dk [\sqrt{2(1 - \cos k|z-z'|)}] e^{-\frac{\gamma}{\eta} k^2(t-t')}, \end{aligned} \quad (33)$$

where $\mu = 1, 2$. The KPZ fixed point relates to the generation of the renormalized term $(\vec{\nabla}h)^2$ as a result of the dynamical evolution of the model. Here $n = \frac{D}{2\pi\gamma K^2}$; for $n > 2$, both U_1 and U_2 decay to zero while for $\frac{1}{2} < n < 2$, only U_2 decays to zero while U_1 keeps growing. The case for $n = 2$ is most interesting in that it leads to a strong coupling fixed point where the U_1 flow diverges, an attribute that gets subsequently reflected in the phase evolution of all relevant quantities like γ , η , D , K and the renormalized parameter λ . This indicates a phase transition from the N^* phase to the SmC^* phase. Unlike in the N^* phase, for each set of γ , η , λ , D and K flows, there is a push-pull mechanism in action. For $\frac{1}{2} < n < 2$, we predict that the system will be in the N^* phase while in the other regions they will flow in the SmC^* phase. This observation supports the experimental observations [28–30] of the N^* - SmC^* phase transition. Figures 1-4 highlight these phase transitions from the N^* phase to the SmC^* phase, focusing on the convergence properties of the flow integrals. The double discontinuities at the points $\kappa = 0.25$ and $\kappa \sim 0.56$ indicate these phase transition points.

NUMERICAL SOLUTION

In order to analyze the detailed temperature dependence of the model, an allusion to the fact that the noise strength D_0 could be related to the Brownian mobility and hence is proportional to $k_B T$, where k_B is the Boltzmann's constant and T is the “effective non-equilibrium temperature” [23, 24, 31, 32] of the system (discussed earlier), we resorted to numerical simulation.

For the actual numerical integration of our 1+1 dimensional model, we used the “forward Euler” discretization scheme with $\Delta t = 10^{-4}$ and $\Delta x = 1$. The Laplacian term in Eq. (4) was discretized within the iterative nearest-neighbor representation, followed on by next-nearest-neighbor, etc. through a recursion loop. In order to ensure dynamic stationarity, the system was dynamically evolved through 10^5 time steps. Diffusion constant $\gamma = 1$ and lattice spacing $a = 1$ were the only fixed parameter values chosen (without any loss of generality). In order to ensure the parameter independence of the fixed points, thereby confirming existence of proper universality classes, we ran simulations over all possible combinations of the following parameter values: $\frac{V_1}{V_2} = 0.1, 1, 10$, $\eta = 1, 10$, $F = 1, 10, : 100$, low noise strength $D = 0.1, 0.5, 1$. Plots are shown only for a few specific choice of these parameter values but the choices as such are arbitrary, since both qualitative and quantitative predictions of the exponent values could be confirmed to remain independent of the choice of parameters. As expected, for even larger values of the noise strength, as also for overly large choices of η , the results trivially converged to the Brownian model or to the “flat, non-rough” stationary limit respectively. Also, we avoided combinations of parameter values (tested through simple dimensional scaling of terms) for which the diffusion, sine-Gordon and noise terms were not sufficiently competitive, as the prediction from the model relies on this competition. For individual asymptotes, e.g. $\gamma \gg V_1, V_2$, or the reverse, the results converged to known fixed points.

In order to clarify the finite sized dependence of this model, lattice sizes of 1000, 10,000 and 100,000 points were used. From our results, we can now safely claim that the universality classes themselves are unaffected by finite sized corrections. The simulation results provide a deeper insight into the dynamical phase transition, the full range of which has hitherto remained elusive to even most updated experimental attempts [28–30].

The scaling regimes depicted in Figures 5 and 6 represent the fixed points defining the corresponding universality classes. The solid line shows a convergence to the value $\alpha \sim 0.5$, $\beta \sim 1/3$ while the dotted line scales as $\alpha \sim 1/3$, $\beta \sim 1/3$. It may be noted that the results shown are block ensemble averages over 10^4 time realizations in each case, and as such are most accurate. Each data point shown is actually a representation of this time/ergodic sampling.

KPZ phase confirmation

Essentially, we are calculating two two-point correlation functions, the spatial correlation function $C_x = \langle [h(x+z, t) - h(z, t)]^2 \rangle$ and the temporal correlation function $C_t = \langle [h(z, t+\tau) - h(z, \tau)]^2 \rangle$. The universality class as such can be confirmed from their respective scaling exponents, the “roughness exponent” α , the “growth exponent” β and the “dynamic exponent” γ . As is well known [2, 4], due to self-affine scaling, such systems can be uniquely expressed by any two of these exponents. e.g. α and z , where $\beta = \frac{\alpha}{z}$.

For large forcing, that is for reasonably large values of $F > 1$, the trajectories converge to a KPZ fixed point characterized by $\alpha \sim 0.5$ and $z \sim 1.5$ [1, 2]. We may add that $F = 1$ is not a special parameter value though. This result confirms the experimental finding of [10, 11]; the term F_0 in our model corresponds to the steady external voltage that was applied to the thin nematic liquid crystal layer in these references.

A conventional strategy employed in some previous works [21, 27] while not availed in others [22] is the incorporation of the KPZ term in the dynamic renormalization structure right from the onset. For the purpose of this manuscript, it is believed to be an incorrect strategy in view of the fact that the later numerical simulation shows the evidence of non-KPZ phases as well. If a KPZ term is added in the starting model itself, this would trivialise the importance of the KPZ convergence for large values of the external forcing.

The “Hidden” phase: Subdiffusive to KPZ

In a remarkable finding, as F decreases from a high value $F \geq 10$ to a relatively lower value e.g. $F = 1$ and below, the system dynamically converges to a “subdiffusive” (SD) universality class characterized by ($\alpha \sim 0.33$, $\beta \sim$

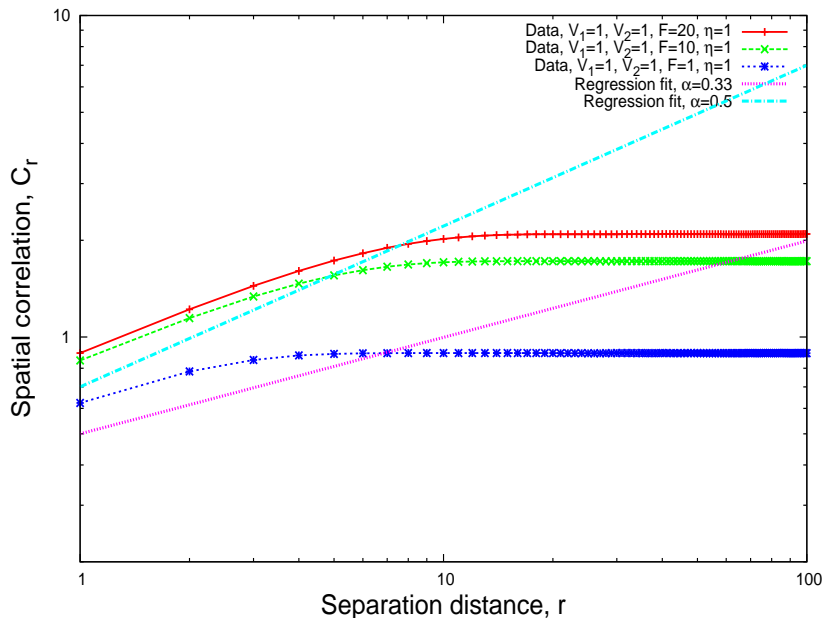


FIG. 5. Spatial correlation function C_x plotted against the spatial separation x in the loglog scale for $V_1 = 1$, $V_2 = 1$, $\eta = 1$, respectively for $F = 1, 10, 20$, as shown in the plots. The results show a remarkable phase transition from the “subdiffusive” phase defined by $\alpha \sim 0.33$, $\beta \sim 0.33$ to a KPZ [1] phase defined by $\alpha \sim 0.5$, $\beta \sim 0.33$. As the ramping force F increases from a relatively low ($F = 1$) to high values ($F = 10, 20$), the system crosses over from a subdiffusive universality class to a KPZ universality class.

0.33, $z \sim 1$). As F is again ramped higher, the trajectories cross over to a KPZ fixed point [1] characterized by ($\alpha \sim 0.5$, $\beta \sim 0.33$, $z \sim 1.5$). Figures 5 and 6 highlight these scaling features and confirms the crossover from the SD to the KPZ phase, and vice versa.

The emergence of an SD phase can be understood from the previously estimated RG flows which define two “jump” transition points at $n = \frac{D\Lambda^2}{2\pi\gamma F^2} = \frac{1}{2}$ and $n = \frac{D\Lambda^2}{2\pi\gamma F^2} = 2$ respectively, as corroborated by the discontinuities at the corresponding points in all the flow integral plots shown in Figs. (1-4). As F increases, $n \rightarrow \frac{1}{2}$ which identifies the KPZ phase in the phase integral plots while with decreasing F , the $n \rightarrow 2$ fixed point is approached. Fig. 5 above clearly shows how the roughness exponent α (defined in [1]) changes from a smoother SD phase, identified by $\alpha \sim 0.33$ to a coarser KPZ phase, characterized by $\alpha \sim 0.5$, thereby leading to a dynamic exponent value of $z \sim 1.5$ in the KPZ phase. These results could be compared with the preroughening-roughening transitions previously noted in [33, 34]. Fig. 5 confirms the values of the “roughness exponent” [1] over a range of F values. The KPZ-growth exponent value remains unchanged for both SD and KPZ dynamics, as is shown in Fig. 6.

The crossover from the SD phase to the KPZ phase has concurrently appeared over this entire parametric range. A crucial feature of this report concerns the prediction of this “hidden phase” and its subsequent transition to the Kardar-Parisi-Zhang (KPZ) phase, as previously reported in experiments [10, 11]. We believe that in this ground breaking experimental study, the SD phase remained elusive due to an inappropriate choice of parameters, attributed to a lack of mechanism to choose parameters over such a wide parameter space. Our model study now presents a structure to arrive at this parameter set whereby such a “hidden” SD phase could be experimentally verified, that at the present, seems to be characterized only by a KPZ dynamics. We have checked the veracity of this prediction for other values of (V_1, V_2), within the range $1 < V_i < 10$ ($i=1, 2$).

From the perspective of quantum spin chains [33] as also in roughening transition, similar multi-phase properties have previously been reported [34], in which the transition from the $n = 1/2$ to the $n = 2$ phase respectively represented a half-integral spin to an integral spin conformation transition, or a pre-roughening to a roughening transition (or a cross-over). These studies also highlight the importance of possible long-ranged phase correlations, and hence spatially controlled transitions [35], that could be studied in the present context as well.

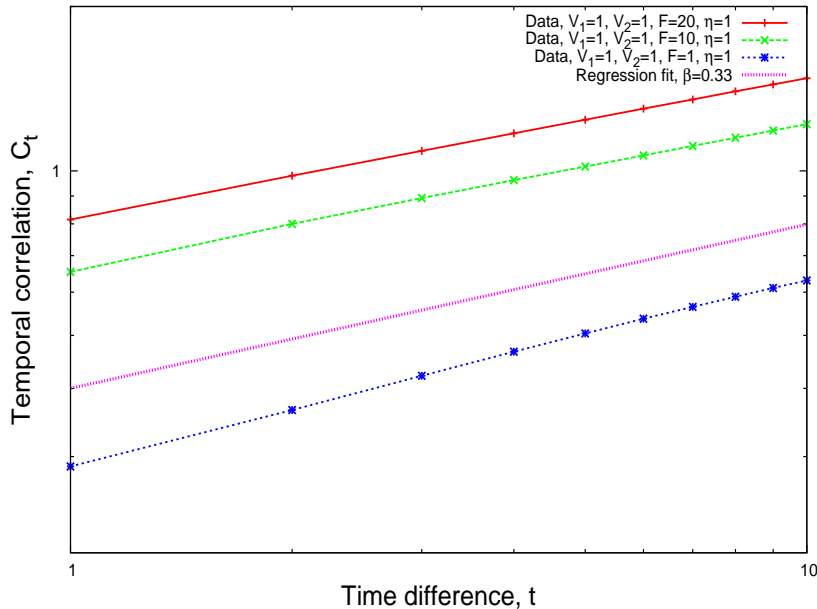


FIG. 6. Temporal correlation function C_t plotted against time difference t in the loglog scale for $V_1 = 1$, $V_2 = 1$, $\eta = 1$, respectively for $F = 1, 10, 20$, as shown in the plots. All gradients converge to the fixed value $\beta \sim 0.33$. The growth exponent is clearly unaffected by the ramping force F .

CONCLUSIONS

Using a complementary combination of analytical (dynamic renormalization group) and numerical techniques, we explore the nonequilibrium scaling features of a stochastically perturbed smectic- C^* liquid crystal that on the one hand confirms known experimental results (prediction of a KPZ phase), while paradigmatically, unearths a “hidden” phase (subdiffusive phase) that has eluded experimentalists thus far.

The prediction of the KPZ universality class from our model, in 1+1 dimensions, validates a recent experimental work by Takeuchi and Sano [11] where they studied the scale-invariant fluctuations of growing interfaces in nematic liquid crystal turbulence. As a perturbed phase, the N^* and SmC^* phases too are expected to behave identically. From a general perspective, for experiments involving more than one spatial dimension, the remit of this model could be easily extended as in [22]. Even for such high-dimensional phases, our model predicts the emergence of a KPZ universality class. Figures 1-4 affirm the transition to the KPZ fixed points noted in these experiments.

A remarkable feature of our numerical analysis is the identification of a hitherto unexplored subdiffusive “smoother” phase characterized by critical exponent values ($\alpha = \frac{1}{3}$, $\beta = \frac{1}{3}$, $z = \frac{\alpha}{\beta} = 1$). We find that this phase flows over to a KPZ phase with vamped up external forcing (F) but otherwise remains dynamically preserved. In other words, this is not a transient feature of this model analysis and should be observable from experiments. We have provided a range of parameter values whereby such a phase could be traced.

Here, we have studied the impact of stochastic fluctuations in modifying the spatiotemporal properties of ferroelectric SmC^* liquid crystals in the presence of an electric field. Our model predicts a first order N^* - SmC^* phase transition, and thereby offers the first theoretical ramification of the experimental observations of a KPZ phase as in [10, 11], with others [28–30] following suit. Our approach extends the remit of the experimental finding of the emergence of a KPZ universality class, showing that other universality classes could also appear, while identifying parameter regimes to look for the same. The implication of finite sized impurities and their contribution in related (likely non-universal) dynamical regimes are likely to enthruse a new generation of material science research, routed in liquid crystals.

-
- [1] Kardar, M., Parisi, G. and Zhang, S. *Dynamic scaling of growing interfaces*. Phys. Rev. Lett. **56**, 889 (1986).
- [2] Barabasi, A. -L. and Stanley, H. E. *Fractal Concepts in Surface Growth*. (Cambridge University Press, 1991).
- [3] Halpin-Healy, T. and Zhang, Y. C. *Kinetic roughening phenomena, stochastic growth, directed polymers and all that. Aspects of multidisciplinary statistical mechanics*. Phys. Rep. **254**, 215 (1995).
- [4] Krug, J. *Origins of scale invariance in growth processes*. Adv. Phys. **46**, 139 (1997).
- [5] Myllys, M., Maunuksela, J., Alava, M. J., Ala-Nissila, T., Merikoski, J., Timonen, J. *Kinetic roughening in slow combustion of paper*. Phys. Rev. E **64**, 036101 (2001).
- [6] Myllys, M., Maunuksela, J., Alava, M. J., Ala-Nissila, T., Timonen, J. *Scaling and noise in slow combustion of paper*. Phys. Rev. Lett. **84**, 1946 (2000).
- [7] Hiller, S., Biradar, A. M., Wrobel, S., Haase, W. *Dielectric behavior at the smectic-C* - chiral-nematic phase transition of a ferroelectric liquid crystal*. Phys. Rev. E **53**, 641 (1996).
- [8] Kumar, S. *Liquid Crystals: Experimental Studies of Physical Properties and Phase Transitions*. (Cambridge University Press (2011)).
- [9] Chattopadhyay, A. K. and Mukherjee, P. K. *Dynamics of cholesteric liquid crystals in the presence of random magnetic fields*. Europhys. Lett. **112**, 60002 (2015).
- [10] Takeuchi, K. A. and Sano, M. *Universal fluctuations of growing interfaces: Evidence in turbulent liquid crystals*. Phys. Rev. Lett. **104**, 230601 (2010).
- [11] Takeuchi, K. A. and Sano, M. *Evidence for geometry-dependent universal fluctuations of the Kardar-Parisi-Zhang interfaces in liquid-crystal turbulence*. J. Stat. Phys. **147**, 853 (2012).
- [12] Golubovic, L. and Wang, Z. G. *Anharmonic Elasticity of Smectics A and Kardar-Parisi-Zhang Model*. Phys. Rev. Lett. **69**, 2535 (1992).
- [13] Golubovic, L. and Wang, Zhen-Gang *Kardar-Parisi-Zhang model and anomalous elasticity of two and three dimensional smectic-A liquid crystals*. Phys. Rev. E **49**, 2567 (1994).
- [14] Geng, Y. et al. *High-fidelity spherical cholesteric liquid crystal Bragg reflectors generating unclonable patterns for secure authentication*. Scientific Rep. **6**, 26840 (2016).
- [15] Slussarenko, S. et al. *Guiding light via geometric phases*. Nature Photonics (2016); doi: 10.1038/nphoton.2016.138.
- [16] Pujolle-Robic, C. and Noirez, L. *Observation of shear-induced nematic-isotropic transition in side-chain liquid crystal polymers*. Nature **409**, 167 (2000).
- [17] van der Kooij, F. M., Kassapidou, K. and Lekkerkerker, H. N. W. *Liquid crystal phase transitions in suspensions of polydisperse plate-like particles*. Nature **406**, 868 (2000).
- [18] Cladis, P. E. and van Saarloos, W. in : Solitons in Liquid Crystals (edited by Lam, and Prost, J.), p. 110, (Springer-Verlog, New York, 1992).
- [19] Modanese, G., *The vacuum state of quantum gravity contains large virtual masses*, Classical and Quantum Gravity **24**(8), 1899 (2007).
- [20] Risken, H. *The Fokker-Planck Equation: Methods of Solution and Applications*. (Springer 2013).
- [21] Nozieres, P. and Gallet, F. *The roughening transition of crystal surfaces. I. static and dynamic renormalization theory, crystal shape and facet growth*. J. Phys. (Paris) **48**, 353 (1987).
- [22] Chattopadhyay, A. K. *The role of pinning and instability in a class of non-equilibrium growth models*. Eur. Phys. J. B **29**, 567 (2002).
- [23] Derrida, B. *Non-equilibrium steady states: Fluctuations and large deviations of the density and of the current*. J. Stat. Mech. 2007, P07023 (2007).
- [24] Jarzynski, C. *Equalities and inequalities: Irreversibility and the second law of thermodynamics at the nanoscale*. Ann. Rev. Cond. Mat. Phys. **2**, 329-351 (2011); *ibid. Diverse phenomena*. Nature Phys. **11**, 105-107 (2015).
- [25] Hohenberg, P. C. and Halperin, B. I. *Theory of dynamic critical phenomena*. Rev. Mod. Phys. **49**, 435 (1977).
- [26] Amit, D. J., Goldschmidt, Y. Y. and Grinstein, S. *Renormalisation group analysis of the phase transition in the 2D Coulomb gas, Sine-Gordon theory and XY-model*. J. Phys. A **13**, 585 (1980).
- [27] Rost, M. and Spohn, H. *Renormalization of the driven sine-Gordon equation in 2+1 dimensions*. Phys. Rev. E **49**, 3709 (1994).
- [28] Patel, J. S. and Goodby, J. W. *Alignment of liquid crystals which exhibit cholesteric to smectic C* phase transitions*. J. Appl. Phys. **59**, 2355 (1986).
- [29] Biradar, A. M. et al. *Switching dynamics of first order phase transition FLCs on a polymer rubbed surface*. Liq. Cryst. **20**, 641 (1996).
- [30] Biradar, A. M. et al. *A sub-hertz frequency dielectric relaxation process in a ferroelectric liquid crystal material*. Liq. Cryst. **27**, 225 (2000).
- [31] Bustamente, C., Liphardt, J. and Ritort, F. *The nonequilibrium thermodynamics of small systems*. Phys. Today **58**, 43-48 (2005);
- [32] Seifert, U. *Stochastic thermodynamics, fluctuation theorems and molecular machines*. Rep. Prog. Phys. **75**, 126001 (2012).
- [33] den Nijs M. and Rommelse, K., *Preroughening transitions in crystal surfaces and valence-bond phases in quantum spin chain*, Phys. Rev. B Cond. Mat. **40**(7), 4709 (1989).
- [34] Park, K. and Kahng, B., *Dynamics of the preroughening transition*, J. Phys. A: Math. and Gen. **26** (12), 2895 (1993).
- [35] Chattopadhyay, A. K., *Nonlocal Kardar-Parisi-Zhang equation with spatially correlated noise*, Phys. Rev. E **60**(1), 293

(1999).